

Magnetization Control and Transfer of Spin-Polarized Cooper Pairs into a Half-Metal Manganite

A. Srivastava,¹ L. A. B. Olde Olthof,^{1,2} A. Di Bernardo,¹ S. Komori,¹ M. Amado,¹ C. Palomares-Garcia,¹ M. Alidoust,³ K. Halterman,⁴ M. G. Blamire,¹ and J. W. A. Robinson^{1,*}

¹*Department of Materials Science and Metallurgy, University of Cambridge, 27 Charles Babbage Road, Cambridge CB3 0FS, United Kingdom*

²*Faculty of Science and Technology and MESA+Institute for Nanotechnology, University of Twente, 7500 AE Enschede, The Netherlands*

³*Department of Physics, K. N. Toosi University of Technology, Tehran 15875-4416, Iran*

⁴*Michelson Lab, Physics Division, Naval Air Warfare Center, China Lake, California 93555, USA*

(Received 1 June 2017; revised manuscript received 19 July 2017; published 17 October 2017)

The pairing state and critical temperature (T_C) of a thin s -wave superconductor (S) on two or more ferromagnets (F) are controllable through the magnetization alignment of the F layers. Magnetization misalignment can lead to spin-polarized triplet-pair creation, and since such triplets are compatible with spin-polarized materials, they are able to pass deeply into the F layers and cause a decrease in T_C . Various experiments on $S/F_1/F_2$ “triplet spin valves” have been performed with the most pronounced suppression of T_C reported in devices containing the half-metal ferromagnet (HMF) CrO_2 (F_2) albeit using out-of-plane magnetic fields to tune magnetic noncollinearity [Singh *et al.*, *Phys. Rev. X* **5**, 021019 (2015)]. Routine transfer of spin-polarized triplets to HMFs is a major goal for superconducting spintronics so as to maximize triplet-state spin polarization. However, CrO_2 is chemically unstable, and out-of-plane fields are undesirable for superconductivity. Here, we demonstrate low-field (3.3 mT) magnetization-tunable pair conversion and transfer of spin-polarized triplet pairs to the chemically stable mixed valence manganite $\text{La}_{2/3}\text{Ca}_{1/3}\text{MnO}_3$ in a pseudo-spin-valve device using in-plane magnetic fields. The results match microscopic theory and offer full control over the pairing state.

DOI: 10.1103/PhysRevApplied.8.044008

I. INTRODUCTION

Superconducting spintronics represents a paradigm for information processing involving the coexistence of spin polarization and superconducting phase coherence [1–3]. Conventional s -wave superconductivity involves the condensation of spin-singlet electron pairs with antiparallel spins. Although singlet pairs are energetically unstable in a ferromagnet, they are able to penetrate a transition-metal ferromagnet (F) at a superconductor-ferromagnet (S/F) interface over distances of a few nanometers [4–10] but without transferring a net spin. Furthermore, singlet pairs are blocked at an S interface with a half-metal ferromagnet (HMF), as there are no available states for one of the two spins of a pair to enter since the Fermi energy for the minority-spin electrons falls within a gap.

Electron pairs in the p -wave superconducting compound Sr_2RuO_4 [11] have parallel spins, and so such spin-triplet pairs carry a net spin in addition to charge. However, the extreme sensitivity of p -wave superconductivity to structural and electronic disorder creates major obstacles to the development of p -wave devices [12]. Spin-triplet pairs with parallel spins but s -wave symmetry may form at

magnetically inhomogeneous s -wave S/F interfaces [1–3]. Since such pairs are compatible with fully spin-polarized materials, their routine creation and transfer to HMFs will open up exciting opportunities for applications in superconducting spintronics where high spin polarization and long spin-flip scattering lengths are desirable.

Spin-polarized triplet pairs form via spin mixing and spin-rotation processes at S/F interfaces [13]. At homogeneously magnetized S/F interfaces or within magnetically collinear $S/F_1/F_2$ spin valves, spin-singlet pairs experience a spatially constant exchange field that acts differentially on the antiparallel spins of a pair, causing transformation to a spin-zero triplet state (spin-mixed state). A rotation of the magnetization at an S/F interface or within an $S/F_1/F_2$ spin valve has the effect of transforming spin-zero triplets to pairs with a parallel projection of spin (spin rotation). For $S/F_1/F_2$ spin valves where S and F_1 (“spin-mixer” layer) are thinner than the spin-singlet coherence length (40 nm in Nb [14] and 1 nm in Co, Fe, and Ni, see Refs. [6,9,10] and [15,16]), spin-polarized triplet-pair creation leads to an effective leakage of superconductivity from S into F_2 and a reduction of the critical temperature (T_C). “Triplet spin valves” (TSVs) are, therefore, sensitive devices for investigating singlet-to-triplet pair conversion [17–20].

*jjr33@cam.ac.uk

Experiments over the past few years have mainly focused on magnetization control of triplet-pair creation in $S/F/S$ Josephson devices and TSVs. In $S/F/S$ devices, various symmetric spin-mixer layers have been added to the S/F interfaces, including rare-earth magnetic spirals [21,22], antiferromagnets [23], Heusler alloys [24], and transition-metal ferromagnets [25–29]. Similarly, in $S/F_1/F_2$ TSVs, $F_{1,2}$ metals [30–34] or F metals (F_1) in combination with the HMF CrO_2 (F_2) [35] have been successfully demonstrated. See, also, the related works on $F/S/F$ spin valves [36–38], spectroscopy experiments on various S/F system experiments [39–49], and also evidence for triplet pairing in graphene on a d -wave superconductor [50].

The most pronounced suppressions of T_C were reported in a $\text{MoGe}/\text{Ni}/\text{Cu}/\text{CrO}_2$ TSV in which out-of-plane magnetic fields created a misalignment between the magnetizations of Ni and CrO_2 [35]; the largest suppression of T_C was close to -800 mK with a constant out-of-plane magnetic field of 2 T. This work extended previous experiments that demonstrated Josephson coupling across CrO_2 [51] (see, also, Refs. [27,36]) in devices that did not contain intentional spin-mixer layers at the S/HMF interfaces. However, CrO_2 is chemically unstable, and so there is a need to identify alternative HMFs in which thin films can be grown and combined with various S/F structures with enhanced chemical stability.

Mixed valence manganites ($\text{La}_{1-x}\text{Ae}_x\text{MnO}_3$, where Ae is an alkaline earth) such as $\text{La}_{1-x}\text{Sr}_x\text{MnO}_3$ and $\text{La}_{2/3}\text{Ca}_{1/3}\text{MnO}_3$ (LCMO) are highly attractive alternatives to CrO_2 since they are chemically stable, and their relatively narrow spin-up and spin-down conduction bands are completely separated leading to HMF behavior at low temperatures [52,53]. In this paper, we report TSV with $\text{Nb}/\text{Cu}/\text{Py}/\text{Au}/\text{LCMO}$ layers in which a nonmonotonic dependence of T_C on the relative magnetization angle (θ) between $\text{Py}(\text{Ni},\text{Fe})$ and LCMO is observed, thus, demonstrating pair conversion and transfer of spin-polarized triplets to LCMO. Recently, we detected Josephson coupling across thin (<30 nm) layers of LCMO [54] but without intentional spin mixers at the S/LCMO interfaces. Related experiments that probe spectroscopic signatures triplet pairing in S/LCMO structures have also been reported [43–45,55] but again without intentional spin-mixer layers. The motivation of the work reported here is to investigate magnetization control of triplet-pair creation and transfer to LCMO, which is fundamental to the development triplet superconductivity based on mixed valence manganites. Furthermore, we want to demonstrate triplet-pair creation in TSVs with small in-plane magnetic fields to avoid complications due to vortices that will be present in TSV that require large out-of-plane magnetic fields.

II. EXPERIMENT

We prepare $\text{Nb}(25\text{nm})/\text{Cu}(5\text{nm})/\text{Py}(3.5\text{nm})/\text{Au}(5\text{nm})/\text{LCMO}(120\text{nm})$ TSVs in several stages. Epitaxial (002)

LCMO is grown from a stoichiometric target by pulse laser deposition (KrF laser, wavelength $\lambda = 248$ nm) on 5×5 mm² single-crystal SrTiO_3 (STO) (001) at a growth temperature of 800°C in flowing N_2O at 130 mTorr with a pulse fluence of 1.5 J/cm² for 15 min and repetition rate of 2 Hz, then 30 min at 3 Hz. The films are annealed *in situ* at the same temperature in oxygen (46 kPa) for 8 h and cooled to room temperature at a rate of $10^\circ\text{C}/\text{min}$. High-resolution x-ray diffraction (see Fig. 1S in the Supplemental Material [56]) confirms single (002) orientation of LCMO with rocking curves on the (002), (004), (006), and (008) Bragg peaks showing full width at half maximum values of 0.12° , 0.18° , 0.209° , and 0.227° , respectively. The c -axis lattice parameter is determined to be 7.670 ± 0.002 Å, consistent with powder diffraction simulations [58]. Au is deposited on LCMO at room temperature using a fluence of 2.5 J/cm² for 3 min at 5 Hz in 30 mTorr of Ar (Au is chosen due to its oxidation resistance and limited solubility with Ni). Au/LCMO bilayers are then transferred in air to an ultra-high-vacuum sputtering system with a base pressure of 3×10^{-9} mBar, and $\text{Nb}/\text{Cu}/\text{Py}$ trilayers are deposited on Au/LCMO in Ar at 1.5 Pa while rotating below stationary magnetrons. The surface of Au is cleaned *in situ* by Ar ion plasma etching (-0.6 -kV extraction energy and 1-kV ion energy) and different etching times in the (0–5)-min range are investigated. During the sputter process, the samples experience a constant in-plane magnetic field of approximately 50 mT.

Control samples of $\text{Au}(5\text{ nm})/\text{LCMO}(120\text{ nm})$ and $\text{Nb}(25\text{ nm})/\text{Cu}(5\text{ nm})/\text{Py}(3.5\text{ nm})/\text{Au}(5\text{ nm})$ are prepared on a 5×5 mm² area STO(001) and single-crystal silicon substrates, respectively, to characterize the isolated magnetic properties of LCMO and Py. Magnetization M vs applied field H is shown in Figs. 1(b) at 10 K. The $M(H)$ of LCMO shows an easy-plane behavior with an in-plane saturation field (H_S) of 50 mT and coercivity (H_C) of 20 mT. In the Supplemental Material [56], we also show (Fig. 4S) that the LCMO is magnetically isotropic in plane at 10 K. In comparison, the Py shows some in plane anisotropy with an easy axis (EA defined as 90°) parallel to the field direction during growth and H_C of 1.8 mT and a harder axis (HA defined as 0°) at a right angle to the EA with $H_C = 1.1$ mT. The volume saturation magnetizations of LCMO and Py are 470 ± 15 emu/cm³ and 650 ± 25 emu/cm³, respectively, which are similar to the values reported elsewhere [for LCMO, see Ref. [59], and see Ref. [60] for Py].

Figure 1(c) shows $M(H)$ of the TSV at 10 K where M is dominated by the 120-nm-thick LCMO layer, and for comparison, the easy-axis $M(H)$ loop is plotted for the $\text{Nb}/\text{Cu}/\text{Py}/\text{Au}$ control [reproduced from Fig. 1(b)]. The $M(H)$ loops show that the TSV magnetization state is parallel (P) beyond ± 30 mT, and a reversal field of -1.8 mT switches the Py moment to achieve an antiparallel (AP) state.

Resistance vs temperature $R(T)$ measurements of the TSVs are performed using a four-point current-bias

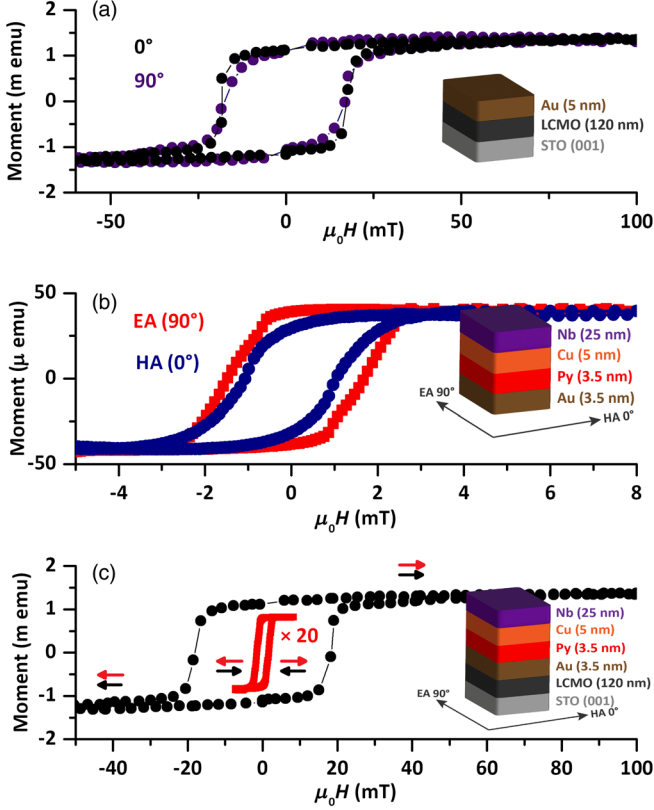


FIG. 1. (a) $M(H)$ loops of LCMO for orthogonal in-plane fields at 10 K. (b) $M(H)$ of Py with the field parallel to the EA and HA. (c) $M(H)$ loop of a complete TSV which is dominated by the magnetization from the 120-nm-thick LCMO, and hence, the Py loop (EA) reproduced from (b) is shown for comparison.

technique on unpatterned samples in a pulse-tube measurement system. The T_C is defined as the temperature corresponding to 50% of the normal-state resistance. We note that care is taken to ensure that the bias current (10 μ A) has no effect on $R(T)$ through the superconducting transition and, therefore, that the T_C is current-bias independent (meaning the bias current is not large enough for vortex-induced voltages to dominate the transport signal). In all cases, $R(T)$ does not show anomalies (e.g., steps) through the superconducting transition.

The effect of the in-plane magnetization configuration on T_C is investigated by measuring $R(T)$ through the superconducting transition as a function of the relative magnetization angle (θ) between LCMO and Py. The $T_C(\theta)$ measurement routine is illustrated in Fig. 2(a) and described as follows: (1) At 10 K, an external field of 100 mT is applied along the HA of Py to magnetize LCMO and Py (along 0°); (2) a magnetic field of -3.3 mT ($< H_C$ of LCMO) is then applied along the HA of Py to reverse the Py moment and obtain the AP state (along 180°) and from $R(T)$ in cooling and warming, $T_C(180^\circ)$ is obtained; (3) the sample warmed to 10 K and rotated in plane to an angle θ in a constant field of amplitude 3.3 mT and from $R(T)$ in cooling and warming $T_C(\theta)$ is obtained. Stage (3) is

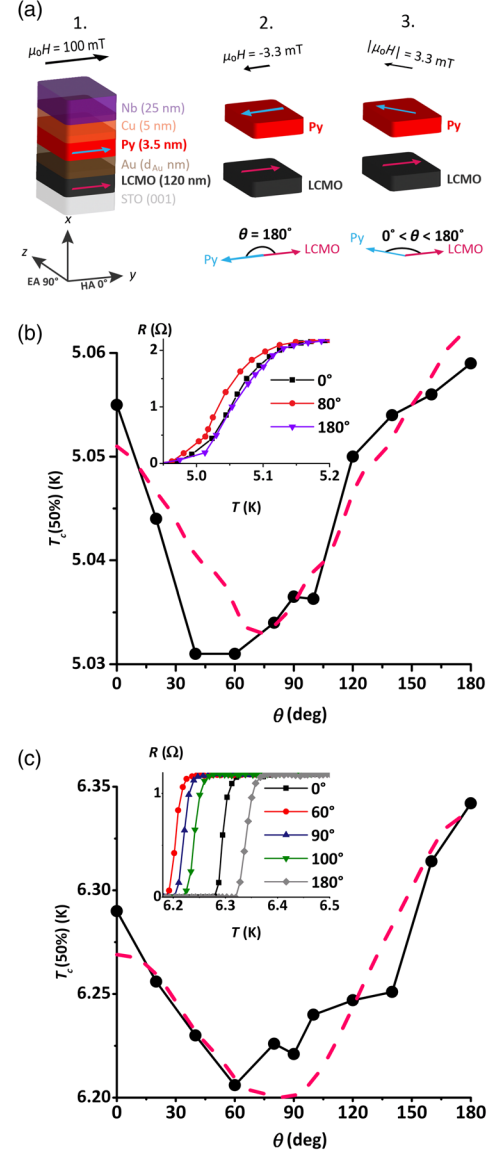


FIG. 2. (a) Measurement sequence to measure T_C as a function of θ . The blue and pink arrows show the likely magnetization configuration of Py and LCMO. (b) and (c) show example data of $T_C(50\%)$ vs θ for Nb(25 nm)/Cu(5 nm)/Py(3.5 nm)/Au(d_{Au})/LCMO(120 nm) TSVs without etching of Au [(b), $d_{Au} = 5$ nm] and following 2 mins of etching [(c), $d_{Au} = 3.75$ nm]. The dashed pink lines show the simulated values of $T_C(50\%)$. The insets show selected $R(T)$ transitions for various magnetization angles (labeled).

repeated at 20° increments to obtain $T_C(\theta)$ between 0° and 180° . We note that a field of -3.3 mT is large enough to fully magnetize Py in all in-plane field directions without altering the remnant state of LCMO.

III. RESULTS AND DISCUSSION

Figure 2(b) shows $T_C(\theta)$ for a TSV in which the Au layer is not etched. Comparing the P and AP states,

we see a standard (albeit small) singlet spin-valve effect with $T_C(\text{AP})-T_C(\text{P})$ close to 10 mK. For angles in the $0^\circ < \theta < 180^\circ$ range, $T_C(\theta)$ decreases to a local minima of 5.32 K, close to $\theta = 60^\circ$ giving a maximum T_C suppression [defined as $\Delta T_C(\theta) = T_C(\text{AP})-T_C(\theta)$] of -28 mK, which is smaller than the average superconducting transition width. To check that $T_C(\theta)$ cannot be attributed to potential effects arising from field nonuniformity on T_C as the TSV is rotated in plane during measurements of $R(T)$ (e.g., if the sample is not mounted perfectly parallel to the applied field), we investigate $T_C(\theta)$ of the Nb(25 nm)/Cu(5 nm)/Py(3.5 nm)/Au(5 nm) control sample with the field applied in plane and tilted out of plane by 10° (see Fig. 2S in the Supplemental Material [56]). A maximum $\Delta T_C(\theta)$ of 10 mK (matching the temperature stability of our system) is observed with no dependence of T_C on θ , meaning that the functional form of $\Delta T_C(\theta)$ in Fig. 2(b) is related to the relative magnetizations of Py and LCMO and not field nonuniformity.

The small maximum value of $\Delta T_C(\theta)$ (-28 mK) seen in Fig. 2(b) indicates low interfacial transparency at the Py/Au or Au/LCMO interfaces, although we note that $R(T)$ does not show anomalous features in the superconducting transition, suggesting a homogeneous interfacial resistance (heterogeneous transparency results in current paths changing direction through the superconducting transition so as to preferentially flow in superconducting regions). To improve the Py/Au interface, we Ar ion etch the Au *in situ* prior to the sputter deposition of Nb/Cu/Py and investigate $\Delta T_C(\theta)$ on etching time (the Au etch rate is 0.75 ± 0.04 nm/min). The largest $\Delta T_C(\theta)$ of -140 mK [Fig. 2(c)] is achieved for an etch time of 2 min with no observable dependence of T_C on θ for an etch time of 8 min. These data indicate that increasing the etch time has the effect of improving the interface transparency between Py and Au with $\Delta T_C(\theta)$ increasing by 110 mK. Simultaneous etching has the effect of enhancing the singlet spin-valve effect with $T_C(\text{AP})-T_C(\text{P})$ increasing from 10 mK (without etching) to 40 mK after 2 min of etching (Fig. 3). Overetching the Au, however, risks introducing roughness and ferromagnetic coupling between Py and LCMO, and so a decrease in $\Delta T_C(\theta)$ beyond a certain etch time is expected (as seen for an etch time of 8 min). We note that we also investigate using Cu as an alternative to Au at the LCMO interface, but only a singlet spin-valve effect is observed [$T_C(\text{AP}) > T_C(\text{P})$]; see the Supplemental Material [56] for further details.

To compare our results to theory, we calculate $\Delta T_C(\theta)$ of the Nb/Cu/Py/Au/LCMO TSVs using a fully microscopic procedure based on numerical solutions to the self-consistent Bogoliubov–de Gennes equations, as extensively discussed in Refs. [18,19,61]. Each layer is assumed to be infinite in the y - z plane [see Fig. 2(a)]. The four interfaces between Nb and LCMO will have differing transparencies, and to account for spin-independent

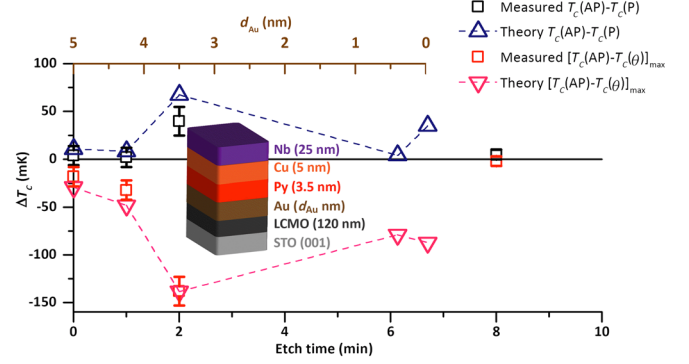


FIG. 3. Theory and experimental ΔT_C vs Au etch time and Au layer thickness.

scattering at these interfaces, we include repulsive δ -function potentials $H_i\delta(x-x_i)$ at each interface position x_i (where $i=1-4$ refers to the interface number; $i=1$ corresponds to the Nb/Cu interface, while $i=4$ refers to the Cu/LCMO interface). The scattering strength is parametrized in dimensionless units by the quantity H_{B_i} written as $H_{B_i} = mH_i/k_F$, where k_F is the Fermi wave vector, and m is the effective mass. Thus, increasing H_{B_i} decreases the interface transparency [18,19]. To effectively characterize the TSV and maintain a tractable parameter space, it is necessary to keep the scattering strength combinations as simple as possible. We find good correlation with experiment when setting $H_{B_1} = H_{B_3} = 0.2$ for the Au/LCMO and Cu/Py interfaces, respectively. For the unetched TSV in Fig. 2(b), we assume a lower transparency at the Py/Au interface with $H_{B_2} = 1.2$, while the Nb/Cu interface is represented with $H_{B_4} = 0.14$. Using these optimized parameters, the model is able to capture the experimental $T_C(\theta)$ behavior seen in Fig. 2. Here the local minima in T_C theoretically relates to the transfer of spin-polarized triplet pairs to LCMO (see, also, the Supplemental Material [56]).

It is interesting to note that the experimental and theoretical minima in $T_C(\theta)$ are shifted from the orthogonal magnetic configuration ($\theta = 90^\circ$). Properly accounting for proximity effects can alter the traditional simple view of the TSV, whereby the equal spin-triplet components undergo a maximum at 90° (leading to a corresponding dip in T_C). By including interface scattering, the quasiparticle amplitudes can undergo phase shifts that push the minimum in T_C away from 90° . The same effect also arises in the ballistic regime [18] from the superposition of quasiparticle interactions with the interfaces and outer system walls that causes equal spin-triplet-pair amplitudes to be largest at relative magnetization angles away from 90° . See, also, Ref. [61] where similar effects are found in the diffusive regime.

In Fig. 3, we compare the experimental and calculated dependence of the maximum value of $\Delta T_C(\theta)$ as a function of etching time. To focus on the effect of the etching time on the Py/Au interface, we fix all interface scattering parameters, except H_{B_2} (relating to the Py/Au interface)

which is allowed to vary in such a way that is consistent with the measured etch rate. Namely, we set $H_{B1} = H_{B3} = 0.4$, $H_{B4} = 0.14$, and $0.7 \leq H_{B2} \leq 1.2$. After a certain time, continued etching is assumed to have no further effect on the interface scattering parameter H_{B2} . The thickness of the Au, however, decreases (0.75 nm/min) with etching. For each datum point, we self-consistently calculate $T_C(\theta)$ and extract ΔT_C and $T_C(\text{AP}) - T_C(\text{P})$. This results in good agreement with the experimental findings. In particular, the spin-valve effect is enhanced for an etching time of 2 min whereby an increased singlet-to-triplet pair conversion takes place. Since the normal-metal layers tend to host spin-polarized triplet pairs, reducing their thickness can also result in a limited T_C reduction that signifies the emergence of spin-polarized triplet pairs.

IV. SUMMARY

We demonstrate triplet-pair creation through magnetization control in Nb/Cu/Py/Cu/LCMO TSVs using in-plane magnetic field as small as 3.3 mT. Efficient pair conversion and spin-polarized triplet-pair transfer to LCMO is achieved for relative magnetization angles between 60° to 90° with a maximum $\Delta T_C(\theta)$ close to -150 mK through band-matching optimization at the Au/LCMO interface. Although $\Delta T_C(\theta)$ is smaller than observed for TSVs containing CrO_2 , which achieves -800 mK [35], in an out-of-plane magnetic field of 2 T, our results agree well with a fully microscopic self-consistent model and demonstrate that the fully spin-polarized and chemically stable mixed valence manganites are highly attractive for superconducting spintronics.

The data sets relating to the figures in this paper are available for access at [62].

ACKNOWLEDGMENTS

This work is funded by the Royal Society (“Superconducting Spintronics”), the Leverhulme Trust (Grant No. IN-2013-033), and the EPSRC through the Programme Grant “Superspin” (Grant No. EP/N017242/1) and the “International network to explore novel superconductivity at advanced oxide superconductor/magnet interfaces and in nanodevices” Grant No. EP/P026311/1 and Doctoral Training Programme (Grant No. EP/M508007/1). J. W. A. R. and A. D. B. acknowledge support from St. John’s College, Cambridge. M. Amado acknowledges support from the European Marie Curie Action MSCA-IFEF-ST No. 656485-Spin3. M. Alidoust is supported by Iran’s National Elites Foundation. K. H. is supported in part by ONR and a grant of HPC resources from the DOD HPCMP.

[1] J. Linder and J. W. A. Robinson, Superconducting spintronics, *Nat. Phys.* **11**, 307 (2015).

- [2] M. Eschrig, Spin-polarized supercurrents for spintronics: A review of current progress, *Rep. Prog. Phys.* **78**, 104501 (2015).
- [3] M. G. Blamire and J. W. A. Robinson, The interface between superconductivity and magnetism: Understanding and device prospects, *J. Phys. Condens. Matter* **26**, 453201 (2014).
- [4] T. Kontos, M. Aprili, J. Lesueur, F. Genêt, B. Stephanidis, and R. Boursier, Josephson Junction through a Thin Ferromagnetic Layer: Negative Coupling, *Phys. Rev. Lett.* **89**, 137007 (2002).
- [5] Y. Blum, A. Tsukernik, M. Karpovski, and A. Palevski, Oscillations of the Superconducting Critical Current in Nb-Cu-Ni-Cu-Nb Junctions, *Phys. Rev. Lett.* **89**, 187004 (2002).
- [6] J. W. A. Robinson, S. Piano, G. Burnell, C. Bell, and M. G. Blamire, Critical Current Oscillations in Strong Ferromagnetic π Junctions, *Phys. Rev. Lett.* **97**, 177003 (2006).
- [7] V. Shelukhin *et al.*, Observation of periodic π -phase shifts in ferromagnet-superconductor multilayers, *Phys. Rev. B* **73**, 174506 (2006).
- [8] F. Born, M. Siegel, E. K. Hollmann, H. Braak, A. A. Golubov, D. Y. Guskova, and M. Y. Kupriyanov, Multiple $0-\pi$ transitions in superconductor/insulator/ferromagnet/superconductor Josephson tunnel junctions, *Phys. Rev. B* **74**, 140501 (2006).
- [9] S. Piano, J. W. A. Robinson, G. Burnell, and M. G. Blamire, $0-\pi$ oscillations in nanostructured Nb/Fe/Nb Josephson junctions, *Eur. Phys. J. B* **58**, 123 (2007).
- [10] J. W. A. Robinson, Z. H. Barber, and M. G. Blamire, Strong ferromagnetic Josephson devices with optimized magnetism, *Appl. Phys. Lett.* **95**, 192509 (2009).
- [11] Y. Maeno, H. Hashimoto, K. Yoshida, S. Nishizaki, T. Fujita, J. G. Bednorz, and F. Lichtenberg, Superconductivity in a layered perovskite without copper, *Nature (London)* **372**, 532 (1994).
- [12] A. P. Mackenzie, R. K. W. Haselwimmer, A. W. Tyler, G. G. Lonzarich, Y. Mori, S. Nishizaki, and Y. Maeno, Extremely Strong Dependence of Superconductivity on Disorder in Sr_2RuO_4 , *Phys. Rev. Lett.* **80**, 161 (1998).
- [13] F. S. Bergeret, A. F. Volkov, and K. B. Efetov, Odd triplet superconductivity and related phenomena in superconductor-ferromagnet structures, *Rev. Mod. Phys.* **77**, 1321 (2005); **77**, 1321 (2005).
- [14] B. W. Maxfield and W. L. McLean, Superconducting penetration depth of niobium, *Phys. Rev.* **139**, A1515 (1965).
- [15] V. V. Ryazanov, Josephson superconductor-ferromagnet-superconductor π -contact as an element of a quantum bit (experiment), *Phys. Usp.* **42**, 825 (1999).
- [16] T. Kontos, M. Aprili, J. Lesueur, and X. Grison, Inhomogeneous Superconductivity Induced in a Ferromagnet by Proximity Effect, *Phys. Rev. Lett.* **86**, 304 (2001).
- [17] Y. V. Fominov, A. A. Golubov, T. Y. Karminskaya, M. Y. Kupriyanov, R. G. Deminov, and L. R. Tagirov, Superconducting triplet spin valve, *JETP Lett.* **91**, 308 (2010).
- [18] K. Halterman and M. Alidoust, Half-metallic superconducting triplet spin valve, *Phys. Rev. B* **94**, 064503 (2016).
- [19] M. Alidoust, K. Halterman, and O. T. Valls, Zero-energy peak and triplet correlations in nanoscale superconductor/ferromagnet/ferromagnet spin valves, *Phys. Rev. B* **92**, 014508 (2015).

- [20] M. Alidoust and K. Halterman, Proximity induced vortices and long-range triplet supercurrents in ferromagnetic Josephson junctions and spin valves, *J. Appl. Phys.* **117**, 123906 (2015).
- [21] J. W. A. Robinson, J. D. S. Witt, and M. G. Blamire, Controlled injection of spin-triplet supercurrents into a strong ferromagnet, *Science* **329**, 59 (2010); see, also, G. B. Halasz, M. G. Blamire, and J. W. A. Robinson, Magnetic-coupling-dependent spin-triplet supercurrents in helimagnet/ferromagnet Josephson junctions, *Phys. Rev. B* **84**, 024517 (2011); J. W. A. Robinson, F. Chiodi, M. Egilmez, Gábor B. Halász, and M. G. Blamire, Supercurrent enhancement in Bloch domain walls, *Sci. Rep.* **2**, 699 (2012).
- [22] J. D. S. Witt, J. W. A. Robinson, and M. G. Blamire, Josephson junctions incorporating a conical magnetic holmium interlayer, *Phys. Rev. B* **85**, 184526 (2012).
- [23] J. W. A. Robinson, N. Banerjee, and M. G. Blamire, Triplet pair correlations and nonmonotonic supercurrent decay with Cr thickness in Nb/Cr/Fe/Nb Josephson devices, *Phys. Rev. B* **89**, 104505 (2014); see, also, J. W. A. Robinson, G. B. Halász, A. I. Buzdin, and M. G. Blamire, Enhanced Supercurrents in Josephson Junctions Containing Nonparallel Ferromagnetic Domains, *Phys. Rev. Lett.* **104**, 207001 (2010).
- [24] D. Sprungmann, K. Westerholt, H. Zabel, M. Weides, and H. Kohlstedt, Evidence for triplet superconductivity in Josephson junctions with barriers of the ferromagnetic Heusler alloy Cu_2MnAl , *Phys. Rev. B* **82**, 060505 (2010).
- [25] T. S. Khaire, M. A. Khasawneh, W. P. Pratt, and N. O. Birge, Observation of Spin-Triplet Superconductivity in Co-Based Josephson Junctions, *Phys. Rev. Lett.* **104**, 137002 (2010).
- [26] C. Klose *et al.*, Optimization of Spin-Triplet Supercurrent in Ferromagnetic Josephson Junctions, *Phys. Rev. Lett.* **108**, 127002 (2012).
- [27] M. S. Anwar, M. Veldhorst, A. Brinkman, and J. Aarts, Long range supercurrents in ferromagnetic CrO_2 using a multilayer contact structure, *Appl. Phys. Lett.* **100**, 052602 (2012).
- [28] N. Banerjee, J. W. A. Robinson, and M. G. Blamire, Reversible control of spin-polarized supercurrents in ferromagnetic Josephson junctions, *Nat. Commun.* **5**, 4771 (2014).
- [29] W. M. Martinez, W. P. Pratt, and N. O. Birge, Amplitude Control of the Spin-Triplet Supercurrent in $S/F/S$ Josephson Junctions, *Phys. Rev. Lett.* **116**, 077001 (2016).
- [30] P. V. Leksin, N. N. Garif'yanov, I. A. Garifullin, Y. V. Fominov, J. Schumann, Y. Krupskaya, V. Kataev, O. G. Schmidt, and B. Buchner, Evidence for Triplet Superconductivity in a Superconductor-Ferromagnet Spin Valve, *Phys. Rev. Lett.* **109**, 057005 (2012).
- [31] V. I. Zdravkov *et al.*, Reentrant superconductivity and superconducting critical temperature oscillations in $F/S/F$ trilayers of $\text{Cu}_{41}\text{Ni}_{59}/\text{Nb}/\text{Cu}_{41}\text{Ni}_{59}$ grown on cobalt oxide, *J. Appl. Phys.* **114**, 033903 (2013).
- [32] X. L. Wang, A. Di Bernardo, N. Banerjee, A. Wells, F. S. Bergeret, M. G. Blamire, and J. W. A. Robinson, Giant triplet proximity effect in superconducting pseudo spin valves with engineered anisotropy, *Phys. Rev. B* **89**, 140508 (2014).
- [33] P. V. Leksin, N. N. Garif'yanov, A. A. Kamashev, Ya. V. Fominov, J. Schumann, C. Hess, V. Kataev, B. Büchner, and I. A. Garifullin, Superconducting spin-valve effect and triplet superconductivity in $\text{CoO}_x/\text{Fe}_1/\text{Cu}/\text{Fe}_2/\text{Cu}/\text{Pb}$ multilayer, *Phys. Rev. B* **91**, 214508 (2015).
- [34] Z. Feng, J. W. A. Robinson, and M. G. Blamire, Out of plane superconducting Nb/Cu/Ni/Cu/Co triplet spin-valves, *Appl. Phys. Lett.* **111**, 042602 (2017).
- [35] A. Singh, S. Voltan, K. Lahabi, and J. Aarts, Colossal Proximity Effect in a Superconducting Triplet Spin Valve Based on the Half-Metallic Ferromagnet CrO_2 , *Phys. Rev. X* **5**, 021019 (2015).
- [36] I. C. Moraru, W. P. Pratt, and N. O. Birge, Magnetization-Dependent T_C Shift in Ferromagnet/Superconductor/Ferromagnet Trilayers with a Strong Ferromagnet, *Phys. Rev. Lett.* **96**, 037004 (2006).
- [37] J. Y. Gu, C.-Y. You, J. S. Jiang, J. Pearson, Y. B. Bazaliy, and S. D. Bader, Magnetization-Orientation Dependence of the Superconducting Transition Temperature in the Ferromagnet-Superconductor-Ferromagnet System: $\text{CuNi}/\text{Nb}/\text{CuNi}$, *Phys. Rev. Lett.* **89**, 267001 (2002).
- [38] Y. Gu, G. B. Halász, J. W. A. Robinson, and M. G. Blamire, Large Superconducting Spin Valve Effect and Ultrasmall Exchange Splitting in Epitaxial Rare-Earth-Niobium Trilayers, *Phys. Rev. Lett.* **115**, 067201 (2015).
- [39] K. A. Yates, L. A. B. Olde Olthof, M. E. Vickers, D. Prabhakaran, M. Egilmez, J. W. A. Robinson, and L. F. Cohen, Andreev bound states in superconductor/ferromagnet point contact Andreev reflection spectra, *Phys. Rev. B* **95**, 094516 (2017).
- [40] A. Di Bernardo, Z. Salman, X. L. Wang *et al.*, Intrinsic Paramagnetic Meissner Effect Due to s -Wave Odd-Frequency Superconductivity, *Phys. Rev. X* **5**, 041021 (2015).
- [41] A. Di Bernardo, S. Diesch, Y. Gu, J. Linder, G. Divitini, C. Ducati, E. Scheer, M. G. Blamire, and J. W. A. Robinson, Signature of magnetic-dependent gapless odd frequency states at superconductor/ferromagnet interfaces, *Nat. Commun.* **6**, 8053 (2015).
- [42] Y. Kalcheim, O. Millo, A. Di Bernardo, A. Pal, and J. W. A. Robinson, Inverse proximity effect at superconductor-ferromagnet interfaces: Evidence for induced triplet pairing in the superconductor, *Phys. Rev. B* **92**, 060501(R) (2015).
- [43] Y. Kalcheim, I. Felner, O. Millo, T. Kirzhner, G. Koren, A. DiBernardo, M. Egilmez, M. G. Blamire, and J. W. A. Robinson, Magnetic field dependence of the proximity-induced triplet superconductivity at ferromagnet/superconductor interfaces, *Phys. Rev. B* **89**, 180506 (2014).
- [44] Y. Kalcheim, O. Millo, M. Egilmez, J. W. A. Robinson, and M. G. Blamire, Evidence for anisotropic triplet superconductor order parameter in half-metallic ferromagnetic $\text{La}_{0.7}\text{Ca}_{0.3}\text{MnO}_3$ proximity coupled to superconducting $\text{Pr}_{1.85}\text{Ce}_{0.15}\text{CuO}_4$, *Phys. Rev. B* **85**, 104504 (2012).
- [45] C. Visani, Z. Sefrioui, J. Tornos, C. Leon, J. Briatico, M. Bibes, A. Barthélémy, J. Santamaría, and J. E. Villegas, Equal-spin Andreev reflection and long-range coherent transport in high-temperature superconductor/half-metallic ferromagnet junctions, *Nat. Phys.* **8**, 539 (2012).
- [46] I. T. M. Usman, K. A. Yates, J. D. Moore *et al.*, Evidence for spin mixing in holmium thin film and crystal samples, *Phys. Rev. B* **83**, 144518 (2011).
- [47] K. M. Boden, W. P. Pratt, and N. O. Birge, Proximity-induced density-of-states oscillations in a superconductor/strong-ferromagnet system, *Phys. Rev. B* **84**, 020510(R) (2011).

- [48] Y. Kalcheim, T. Kirzhner, G. Koren, and O. Millo, Long-range proximity effect in $\text{La}_{2/3}\text{Ca}_{1/3}\text{MnO}_3/(100)\text{YBa}_2\text{Cu}_3\text{O}_{7-\delta}$ ferromagnet/superconductor bilayers: Evidence for induced triplet superconductivity in the ferromagnet, *Phys. Rev. B* **83**, 064510 (2011).
- [49] P. SanGiorgio, S. Reymond, M. R. Beasley, J. H. Kwon, and K. Char, Anomalous Double Peak Structure in Superconductor/Ferromagnet Tunneling Density of States, *Phys. Rev. Lett.* **100**, 237002 (2008).
- [50] A. Di Bernardo *et al.*, p-wave triggered superconductivity in single-layer graphene on an electron-doped oxide superconductor, *Nat. Commun.* **8**, 14024 (2017).
- [51] R. S. Keizer, S. T. B. Goennenwein, T. M. Klapwijk, G. Miao, G. Xiao, and A. Gupta, A spin triplet supercurrent through the half-metallic ferromagnet CrO_2 , *Nature (London)* **439**, 825 (2006).
- [52] J. Y. T. Wei, N.-C. Yeh, and R. P. Vasquez, Tunneling Evidence of Half-Metallic Ferromagnetism in $\text{La}_{0.7}\text{Ca}_{0.3}\text{MnO}_3$, *Phys. Rev. Lett.* **79**, 5150 (1997).
- [53] Y. Okimoto, T. Katsufuji, T. Ishikawa, A. Urushibara, T. Arima, and Y. Tokura, Anomalous Variation of Optical Spectra with Spin Polarization in Double-Exchange Ferromagnet: $\text{La}_{1-x}\text{Sr}_x\text{MnO}_3$, *Phys. Rev. Lett.* **75**, 109 (1995).
- [54] M. Egilmez, J. W. A. Robinson, J. L. MacManus-Driscoll, L. Chen, H. Wang, and M. G. Blamire, Supercurrents in half-metallic ferromagnetic $\text{La}_{0.7}\text{Ca}_{0.3}\text{MnO}_3$, *Europhys. Lett.* **106**, 37003 (2014).
- [55] C. Visani, F. Cuellar, A. Pérez-Muñoz, Z. Sefrioui, C. Leon, J. Santamaria, and J. E. Villegas, Magnetic field influence on the proximity effect at $\text{YBa}_2\text{Cu}_3\text{O}_7/\text{La}_{2/3}\text{Ca}_{1/3}\text{MnO}_3$ superconductor/half-metal interfaces, *Phys. Rev. B* **92**, 014519 (2015).
- [56] See Supplemental Material at <http://link.aps.org/supplemental/10.1103/PhysRevApplied.8.044008> for further information on the structural and magnetic properties of the spin valve and additional numerical details of the microscopic framework used, which includes Ref. [56].
- [57] R. Yang, X. M. Li, W. D. Yu, X. D. Gao, D. S. Shang, X. J. Liu, X. Cao, Q. Wang, and L. D. Chen, The polarity origin of the bipolar resistance switching behaviors in metal/ $\text{La}_{0.7}\text{Ca}_{0.3}\text{MnO}_3$ /Pt junctions, *Appl. Phys. Lett.* **95**, 072105 (2009).
- [58] P. R. Sagdeo, S. Anwar, and N. P. Lalla, Powder x-ray diffraction and Rietveld analysis of $\text{La}_{1-x}\text{Ca}_x\text{MnO}_3$, *Powder Diffr.* **21**, 40 (2006).
- [59] S. Valencia, Z. Konstantinovic, D. Schmitz, A. Gaupp, L. Balcells, and B. Martínez, Interfacial effects in manganite thin films with different capping layers of interest for spintronic applications, *Phys. Rev. B* **84**, 024413 (2011).
- [60] A. Wallraff, D. I. Schuster, A. Blais, L. Frunzio, J. Majer, M. H. Devoret, S. M. Girvin, and R. J. Schoelkopf, Reducing the critical current for short-pulse spin-transfer switching of nanomagnets, *Appl. Phys. Lett.* **87**, 112507 (2005).
- [61] P. H. Barsic, O. T. Valls, and K. Halterman, Thermodynamics and phase diagrams of layered superconductor/ferromagnet nanostructures, *Phys. Rev. B* **75**, 104502 (2007).
- [62] DOI: 10.17863/CAM.13096.